



THE UNIVERSITY *of* EDINBURGH

Edinburgh Research Explorer

Cross-species efficacy of enzyme replacement therapy for CLN1 disease in mice and sheep

Citation for published version:

Nelvagal, HR, Eaton, S, Wang, SH, Eultgen, EM, Takahashi, K, Le, SQ, Nesbitt, R, Dearborn, JT, Siano, N, Puhl, AC, Dickson, PI, Thompson, G, Murdoch, F, Brennan, P, Gray, M, Greenhalgh, S, Tennant, P, Gregson, R, Clutton, E, Nixon, J, Proudfoot, C, Guido, S, Lillico, S, Whitelaw, B, Lu, J-Y, Hofmann, SL, Ekins, S, Sands, MS, Wishart, T & Cooper, JD 2022, 'Cross-species efficacy of enzyme replacement therapy for CLN1 disease in mice and sheep', *Journal of Clinical Investigation*.
<https://doi.org/10.1172/JCI163107>

Digital Object Identifier (DOI):

[10.1172/JCI163107](https://doi.org/10.1172/JCI163107)

Link:

[Link to publication record in Edinburgh Research Explorer](#)

Document Version:

Publisher's PDF, also known as Version of record

Published In:

Journal of Clinical Investigation

General rights

Copyright for the publications made accessible via the Edinburgh Research Explorer is retained by the author(s) and / or other copyright owners and it is a condition of accessing these publications that users recognise and abide by the legal requirements associated with these rights.

Take down policy

The University of Edinburgh has made every reasonable effort to ensure that Edinburgh Research Explorer content complies with UK legislation. If you believe that the public display of this file breaches copyright please contact openaccess@ed.ac.uk providing details, and we will remove access to the work immediately and investigate your claim.



Cross-species efficacy of enzyme replacement therapy for CLN1 disease in mice and sheep

Hemanth R. Nelvagal, ... , Thomas M. Wishart, Jonathan D. Cooper

J Clin Invest. 2022. <https://doi.org/10.1172/JCI163107>.

Research [In-Press Preview](#) [Neuroscience](#) [Therapeutics](#)

Graphical abstract

□

Find the latest version:

<https://jci.me/163107/pdf>



Title:

Cross-species efficacy of enzyme replacement therapy for CLN1 disease in mice and sheep

Authors:

Hemanth R. Nelvagal^{1**}, Samantha L. Eaton^{2**}, Sophie H. Wang¹, Elizabeth M. Eultgen¹, Keigo Takahashi¹, Steven Q. Le¹, Rachel Nesbitt³, Joshua T. Dearborn³, Nicholas Siano⁴, Ana C. Puhl⁵, Patricia I. Dickson^{1,6}, Gerard Thompson^{7,8}, Fraser Murdoch², Paul M Brennan^{7,8}, Mark Gray^{2,9}, Stephen N Greenhalgh^{2,9}, Peter Tennant^{2,9}, Rachael Gregson^{2,9}, Eddie Clutton^{2,9}, James Nixon^{2,9}, Chris Proudfoot^{2,9}, Stefano Guido², Simon G. Lillico², C. Bruce A. Whitelaw², Jui-Yun Lu^{10‡}, Sandra L Hofmann¹⁰, Sean Ekins⁵, Mark S Sands^{3,6}, Thomas M Wishart^{2†}, Jonathan D. Cooper^{1,6,11†*}

Affiliations:

¹Department of Pediatrics, Washington University in St Louis, School of Medicine, 660 S Euclid Ave, St Louis, MO 63110, USA

²The Roslin Institute and Royal (Dick) School of Veterinary Studies, University of Edinburgh, Easter Bush Campus, Easter Bush, EH25 9RG, Scotland, UK.

³Department of Medicine, Washington University in St Louis, School of Medicine, 660 S Euclid Ave, St Louis, MO 63110, USA

⁴Discovery Science Division, Amicus Therapeutics, Inc., 3675 Market St, Philadelphia, PA 19104, USA.

⁵Collaborations Pharmaceuticals, Inc. 840 Main Campus Drive, Lab 3510, Raleigh, NC 27606, USA

⁶Department of Genetics, Washington University in St Louis, School of Medicine, 660 S Euclid Ave, St Louis, MO 63110, USA

⁷Centre for Clinical Brain Sciences, University of Edinburgh, Chancellor's Building, 49 Little France Crescent, Edinburgh, EH16 4SB, Scotland, UK

⁸Department of Clinical Neurosciences, NHS Lothian, 50 Little France Crescent, Edinburgh, EH16 4TJ, Scotland, UK

⁹The Large Animal Research & Imaging Facility (LARIF), Royal (Dick) School of Veterinary Studies, University of Edinburgh, Easter Bush Campus, Easter Bush, EH25 9RG, Scotland, UK.

¹⁰Department of Internal Medicine, University of Texas Southwestern Medical Center, 5323 Harry Hines Blvd, Dallas, TX 75390, USA

¹¹Department of Neurology, Washington University in St Louis, School of Medicine, 660 S Euclid Ave, St Louis, MO 63110, USA

** These authors contributed equally

† These authors contributed equally

‡Current contact information: *juiyun.lu@gmail.com*

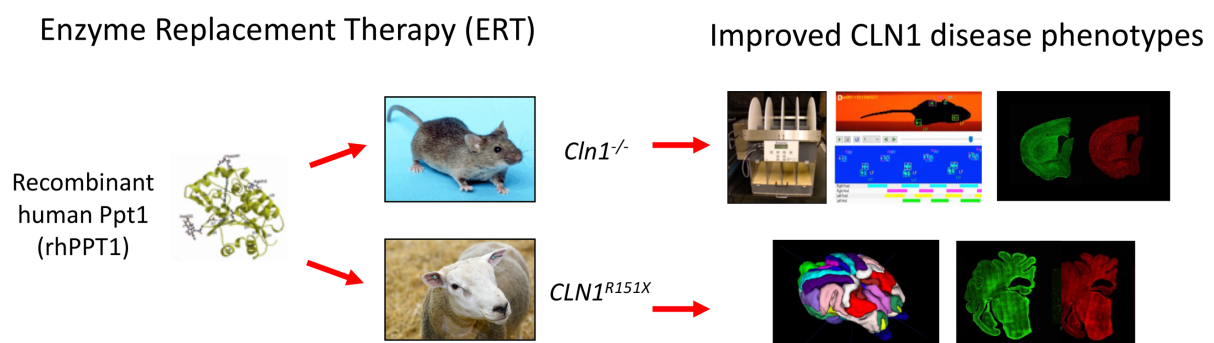
***Author for correspondence:** Jonathan D. Cooper, Departments of Pediatrics, Genetics and Neurology, Washington University in St Louis, School of Medicine, 660 S Euclid Ave, St Louis, MO 63110, USA. Phone: +1 (314) 273-9067. Fax +1 (314) 286-2894. E-mail: *cooperjd@wustl.edu*

One Sentence Summary: Repeated dosing of enzyme replacement therapy with recombinant human PPT1 ameliorates CNS disease phenotypes in mouse and sheep models of CLN1 disease.

Abstract:

CLN1 disease is a fatal neurodegenerative lysosomal storage disorder resulting from mutations in the *CLN1* gene encoding the soluble lysosomal enzyme, palmitoyl-protein thioesterase-1 (PPT1). Therapies for CLN1 disease have proven challenging because of the aggressive disease course and the need to treat widespread areas of the brain and spinal cord. Indeed, gene therapy has proven less effective for CLN1 disease than for other similar lysosomal enzyme deficiencies. We therefore tested the efficacy of enzyme replacement therapy (ERT) by delivering monthly infusions of recombinant human PPT1 (rhPPT1) in PPT1-deficient mice (*Cln1*^{-/-}), and *CLN1*^{R151X} sheep to assess scale up for translation. In *Cln1*^{-/-} mice, intracerebroventricular rhPPT1 delivery was the most effective route of administration, resulting in therapeutically relevant CNS levels of PPT1 activity. rhPPT1 treated-mice had improved motor function, reduced disease-associated pathology, and diminished neuronal loss. In *CLN1*^{R151X} sheep, intracerebroventricular infusions resulted in widespread rhPPT1 distribution and positive treatment effects measured by quantitative structural magnetic resonance imaging and neuropathology. These findings demonstrate the feasibility and therapeutic efficacy of intracerebroventricular rhPPT1 enzyme replacement therapy. This represents a key step towards clinical testing of ERT in children with CLN1 disease and highlights the importance of a cross-species approach to developing a successful treatment strategy.

Graphical Abstract



Main Text:

INTRODUCTION

In contrast to other monogenic causes of neurodegeneration such as mitochondrial and peroxisomal disease (1, 2), the majority of fatal lysosomal storage disorders (LSDs) are caused by a deficiency in proteins that are amenable to exogenous supply (3). These are soluble lysosomal enzymes that can be secreted and taken up by cells via mannose-6-phosphate receptors, in a process named ‘cross-correction’ (4). Nonetheless, the blood-brain barrier prevents systemically delivered enzyme replacement therapy (ERT) from reaching the central nervous system (CNS), unless its uptake properties are modified (5).

Intracerebroventricular delivery of recombinant enzyme is therefore an attractive option to overcome this problem and deliver ERT directly to the brain. However, across over more than 40 neuronopathic LSDs, only one has an approved treatment available (6), so CNS-directed ERT still lacks general principles and procedures. Obstacles to developing ERT include manufacturing appropriately glycosylated and phosphorylated recombinant enzymes, defining appropriate dosing regimens, and delivering enzymes to reach all affected CNS regions (3). Importantly, there is a particular unmet need to scale up pre-clinical advances made in mouse models to large animal models to maximize the chances of successful clinical translation.

CLN1 disease, also called infantile neuronal ceroid lipofuscinosis or infantile Batten disease, is a rapidly progressing, devastating neurodegenerative LSD (7). The classic form of CLN1 disease has an infantile onset and can present as early as six months of age. However, some mutations in this gene result in more delayed presentations according to the precise mutation (8, 9). Its clinical manifestations include sensory and motor deficits, visual impairment leading to blindness, and epileptic seizures (10). Because there is currently no effective

therapy, all cases are fatal (11, 12), with a life expectancy of nine to twelve years (10). This disease results from mutations in the *CLN1* gene that encodes the soluble lysosomal enzyme palmitoyl protein thioesterase-1 (PPT1) (9, 13). Although CLN1 disease is theoretically amenable to an ERT strategy, developing this approach represents a greater challenge than other LSDs. This is due to its early onset and aggressive disease course, and the need to treat widespread regions of the CNS including both brain and spinal cord (14, 15).

We have previously shown that administration of a single intrathecal or intravenous dose of recombinant human PPT1 (rhPPT1) to neonatal PPT1-deficient mice (*Cln1^{-/-}*) produced modest effects on behavior and pathology (16-18). Because exogenously supplied rhPPT1 has a finite half-life (16), we hypothesized that repeated dosing of the central nervous system would be required to provide a translatable therapy.

In this study, we tested this repeated dosing strategy first in *Cln1^{-/-}* mice, a well-established and characterized model recapitulating most aspects of classical CLN1 disease (14, 15, 19), using a previously defined dose and frequency based on enzyme half-life (16). We then applied the same strategy to a recently generated sheep model of CLN1 disease (20), carrying the most common human disease-causing null mutation (*CLN1^{R151X}*). This used infusion parameters similar to those used in other large animal models of LSDs (21, 22). This novel sheep model allowed assessment of enzyme biodistribution and dosing in a species with a brain size and complexity that approximates that of the human brain.

We determined the therapeutic efficacy of intracerebroventricular delivery of rhPPT1 into the cerebrospinal fluid (CSF) in *Cln1^{-/-}* mice. In addition to the well-characterized brain pathology in CLN1 disease, we recently highlighted the involvement of the spinal cord early

in disease progression (15, 23). Therefore, we also compared the efficacy of intrathecal delivery into the lumbosacral space, and a combined dual delivery approach combining intracerebroventricular and intrathecal infusions of the same total dose of enzyme to determine the best route of administration in *Cln1*^{-/-} mice, before moving to test rhPPT1 in sheep.

Our data show that repeated dosing of rhPPT1 is an effective therapy in CLN1 disease animal models across different species. These results represent a key step towards clinical testing of ERT in children with CLN1 disease.

RESULTS

***In vitro* characterization and intracerebroventricular delivery of rhPPT1**

The rhPPT1 used in this study was expressed and purified as previously described (17), and on western blotting showed a molecular weight just below 37 kDa (**Figure 1A**), consistent with the previously reported migration of rhPPT1 as a 34 kDa band in an SDS-PAGE gel (17). To ensure that this rhPPT1 preparation had properties appropriate for *in vivo* use, we performed additional biochemical characterization of the enzyme. The half-maximal binding (K_d) of rhPPT1 to the mannose-6-phosphate receptor was 2.8 nM (**Figure 1B**).

Approximately 64% of the total rhPPT1 loaded onto a cation independent mannose-6-phosphate receptor affinity column was retained on the column (**Figure 1C**). Analysis of site-specific glycosylation revealed that asparagine residues Asn170, Asn185, and Asn205 were highly glycosylated. Asn170 contained 29% bisphosphorylation and 15% monophosphorylation, Asn185 was 71% monophosphorylated, and Asn205 contained 23%

bisphosphorylation and 36% monophosphorylation. These biochemical properties are favorable for the binding and uptake of our rhPPT1 and its use in an ERT strategy.

We next tested the capability of monthly intracerebroventricular infusions of 20 μ g of rhPPT1 (5 μ l of a 4 mg/ml solution) to increase the level of enzymatically active PPT1 in the CNS of *Cln1*^{-/-} mice. This dose and infusion frequency in mice were chosen based on our previous dose-response studies following a single intrathecal infusion of rhPPT1 in *Cln1*^{-/-} mice (16), and the relative persistence of PPT1 enzyme activity within the CNS (16).

In the current study, brain and spinal cord tissue were collected 24 h after the final infusion at six months. Intracerebroventricular delivery of rhPPT1 resulted in a statistically significant increase in PPT1 activity within the CNS of *Cln1*^{-/-} mice when compared to vehicle-treated controls, which showed virtually undetectable levels of PPT1 activity (**Figure 1D**). This elevation in PPT1 activity was seen both in the brain (~64% of WT) and spinal cord (~38% of WT) of rhPPT1-treated mice. We previously showed that a reduction in the secondary elevation of other lysosomal enzymes that accompanies PPT1 deficiency can serve as a biochemical surrogate of therapeutic response in *Cln1*^{-/-} mice (23, 24). Six-month-old vehicle-treated *Cln1*^{-/-} mice had elevated levels of β -glucuronidase activity compared to wild-type controls. β -glucuronidase activity was statistically significantly reduced in *Cln1*^{-/-} mice receiving intracerebroventricular rhPPT1 infusions compared to their vehicle-treated counterparts (**Fig. 1E**).

Intracerebroventricular administration of rhPPT1 significantly improves motor performance in *Cln1*^{-/-} mice

We first determined whether monthly intracerebroventricular infusions of the same 20 μ g dose of rhPPT1 would ameliorate previously characterized behavioral and neuropathological phenotypes in *Cln1*^{-/-} mice. Semi-automated gait analysis revealed that intracerebroventricular vehicle-treated *Cln1*^{-/-} mice displayed an early period of hypermobility followed by a general decline in overall mobility starting at 4 months, with statistically significant effects on overall speed, cadence, and limb movement (**Figure 2A**). This performance is comparable to our previous gait analysis data from untreated *Cln1*^{-/-} mice (15, 23). In contrast, the intracerebroventricular rhPPT1-treated group had improved gait performance. There were statistically significant differences between the intracerebroventricular rhPPT1-treated and intracerebroventricular vehicle-treated groups across most gait parameters, with intracerebroventricular rhPPT1-treated *Cln1*^{-/-} mice showing an overall gait performance more like wild-type controls (**Figure 2A**).

We previously demonstrated decreased rotarod performance of *Cln1*^{-/-} mice as compared to wild-type controls beginning at five months of age (25, 26). Therefore, we also tested wild-type, intracerebroventricular rhPPT1-treated and intracerebroventricular vehicle-treated *Cln1*^{-/-} mice on both stationary and constant speed rotarod paradigms. In the constant speed rotarod test, both intracerebroventricular rhPPT1- and vehicle-treated groups showed impaired performance at five and six months as compared to their wild-type counterparts (**Figure 2B**), but this was not statistically significant. In contrast, in the stationary paradigm, while intracerebroventricular vehicle-treated mice showed a statistically significantly shorter time to fall at six months (**Figure 2B**), intracerebroventricular rhPPT1-treated mice performed as well as their wild-type counterparts.

Intracerebroventricular administration of rhPPT1 significantly attenuates *Cln1*^{-/-} neuropathology

The brains and spinal cords of intracerebroventricular rhPPT1- and vehicle-treated mice were analyzed for neuropathological markers in well-established regions of known pathology.

These include the primary somatosensory barrel field (S1BF), ventral posterior nuclei of the thalamus (VPM/VPL), and the ventral horn of the cervical and lumbo-sacral spinal cord (14, 15). Vehicle-treated *Cln1*^{-/-} mice had statistically significantly elevated levels of activated astrocytes (**Figure 3A**) and microglia (**Figure 3B**) across all central nervous system regions.

This was statistically significantly reduced in intracerebroventricular rhPPT1-treated *Cln1*^{-/-} mice (**Figures 3A, B**). Similarly, the statistically significantly increased levels of

intralysosomal subunit C of mitochondrial ATP synthase (SCMAS) present in all central nervous system regions in the vehicle-treated group were statistically significantly reduced in the intracerebroventricular rhPPT1-treated group (**Figure 4A**). Statistically significant neuron loss and cortical atrophy is observed in the brains and spinal cords of *Cln1*^{-/-} mice at end-stage (14, 15, 23, 27) and was also seen in intracerebroventricular vehicle-treated *Cln1*^{-/-} mice with statistically significantly fewer neurons in the brain and cord. In contrast, intracerebroventricular rhPPT1-treated mice showed statistically significantly reduced neuron loss across all regions (**Figure 4B**). These intracerebroventricular rhPPT1-treated mice also showed statistically significantly less cortical atrophy (**Figure 4C**) compared to the intracerebroventricular vehicle-treated controls.

Alternate delivery routes are not as effective as intracerebroventricular delivery alone

The spinal cord is severely affected in *Cln1*^{-/-} mice, starting in the early stages of disease progression (15, 16, 23). Therefore, we also tested whether delivering monthly intrathecal (IT) injections of the same 20 µg dose of rhPPT1 to *Cln1*^{-/-} mice would improve the treatment outcomes compared to intracerebroventricular infusions alone. We also tested a dual delivery strategy by infusing the same total 20 µg dose of rhPPT1 via both intracerebroventricular and intrathecal routes, with half the dose (10 µg or 2.5µl of 4mg/ml rhPPT1) delivered via each route.

For both intrathecal rhPPT1-treated mice as well a combination intracerebroventricular and intrathecal rhPPT1 delivery there was a statistically significant increase in PPT1 enzyme activity in the brain and spinal cords of *Cln1*^{-/-} mice (**Figure S1A**) and a decrease in β-glucuronidase activity (**Figure S1B**), as compared to vehicle treated controls. Intrathecal rhPPT1-treated mice outperformed intrathecal vehicle-treated *Cln1*^{-/-} mice at six months on the stationary rotarod, and at five and six months on the constant speed rotarod (**Figure S2B**). However, dual delivery of rhPPT1 via both intracerebroventricular and intrathecal rhPPT1 did not show statistically significant treatment effects in either rotarod test (**Figure S2B, S3B**). Furthermore, compared to intracerebroventricular rhPPT1-treated mice, both intrathecal delivery alone and dual delivery of rhPPT1 had less impact upon the gait performance of *Cln1*^{-/-} mice (**Figure S2A, S3A**).

Using neuropathological outcome measures, intrathecal administration of rhPPT1 and dual delivery rhPPT1-treated *Cln1*^{-/-} mice displayed a variety of treatment effects, some of which were statistically significantly different from vehicle-treated controls. These effects varied across central nervous system regions and varied for astrocytosis (**Figure S4A**), microglial activation (**Figure S4B**), storage material accumulation (**Figure S5A**), neuron survival and

cortical thickness (**Figure S5B**). However, neither of these alternative delivery routes showed a comparable level of rescue across all pathological phenotypes as that provided by ICV administration of rhPPT1 alone.

Intracerebroventricular administration of rhPPT1 in *CLNI^{R151X}* sheep

We next sought to scale up the repeated intracerebroventricular rhPPT1 dosing strategy in a larger and more complex central nervous system. We first confirmed that a single dose of rhPPT1 would elevate PPT1 activity in the central nervous system of the recently generated *CLNI^{R151X}* sheep model (20). Four, six-month-old homozygous *CLNI^{R151X}* sheep were infused with a single dose of rhPPT1. The scaled up dose of 4 mg rhPPT1 (1 ml total volume of the same 4 mg/ml enzyme preparation used in *ClnI^{-/-}* mice) was based upon practical considerations of the volume and rate of infusion, while minimizing anesthetic risk, and was delivered using infusion parameters similar to those used when delivering ERT to TPP1 deficient dogs (21, 22).

Sheep that received a single 4mg dose of intracerebroventricular rhPPT1 were sacrificed at twenty-four hours, one week, two weeks, and one month after the infusion. PPT1 activity in the CSF was found to be increased to 92% of WT activity 24 h post-administration. Thereafter, it dropped to 7%, 3% and 3% at 1 week, 2 week and 1 month post-dosing, respectively. At 24 h, PPT1 activity was elevated across multiple brain regions including the subventricular zone (12.6% of WT), cortex (1.1% of WT), midbrain (0.9% of WT) and brainstem (2.9% of WT). This level of PPT1 activity progressively decreased in animals sacrificed at one week, two weeks and one month after infusion (**Figure S6**).

To test the therapeutic efficacy of intracerebroventricular rhPPT1, six-month-old (early symptomatic) homozygous *CLNI^{R151X}* sheep (20) (n = 2) received monthly intracerebroventricular infusions for seven months of 4 mg rhPPT1 from the same batch of enzyme as that used in *ClnI^{-/-}* mice (1 ml of 4 mg/ml for each infusion), using the same infusion ports and parameters previously used when delivering rhTPP1 to CLN2 deficient dogs (21, 22). The rhPPT1-treated *CLNI^{R151X}* sheep were sacrificed at 13 months of age, along with two age-matched WT and two untreated *CLNI^{R151X}* sheep. The CSF levels in rhPPT1 treated sheep showed increases of up to 150% of WT PPT1 enzyme activity levels at 1 week post final administration of the rhPPT1 (**Figure S6**).

All sheep underwent structural magnetic resonance imaging of the brain within 1 hour after being sacrificed, allowing the removal of the metal ports used for transfusions. Cortical grey matter regions undergo differential degrees of atrophy in *CLNI^{R151X}* homozygous animals (20). Gross anatomical examination of brains collected at autopsy revealed pronounced cerebral and cerebellar atrophy in untreated *CLNI^{R151X}* sheep compared to wild-type brains. In contrast, rhPPT1-treated *CLNI^{R151X}* sheep brains displayed less atrophy of both the forebrain and cerebellum (**Figure 5A**). A similar protective effect of rhPPT1 administration was observed in magnetic resonance imaging (MRI) analysis of the rhPPT1-treated *CLNI^{R151X}* sheep (**Figure 5B**). To assess the relative preservation of cortical regions, even in the presence of underlying grey matter atrophy we normalized regional grey matter volumes to total grey matter volume (**Summarized in Data File S1, Supplementary Table 1**). After atlas-based segmentation, histograms of the thickness of individual cortical regions were compared across experimental groups in each of 18 neocortical structures from the INRA atlas (28), (**Data file S3**). This revealed a range of positive treatment effects upon cortical thickness in most cortical regions, with a shift in thickness histograms closer to WT values in

rhPPT1-treated *CLNI^{R151X}* sheep (**Figure 5C**, with data from all regions in **Data File S3**). These effects were not uniform across all cortical regions (**Figure 5D**), being more pronounced rostrally than in caudal cortical areas, with a few regions not benefiting from rhPPT1 treatment (data from all regions **Summarized in Data File S1, Supplementary Table 1**).

We also performed a neuropathological analysis of wild-type, untreated *CLNI^{R151X}* sheep, and rhPPT1-treated *CLNI^{R151X}* sheep brains. We analyzed previously identified affected brain regions (20) including the primary somatosensory cortex, both at the level of the intracerebroventricular catheter (located in the rostral somatosensory cortex) and of the thalamus (the caudal somatosensory cortex), in addition to the thalamus itself. There was an overall reduction in astrogliosis, microglial activation, and autofluorescent storage material accumulation (**Figure 6A**) in the rhPPT1-treated *CLNI^{R151X}* sheep compared to the untreated *CLNI R151X* sheep. The thickness of the primary somatosensory cortex was moderately increased in rhPPT1-treated *CLNI^{R151X}* sheep as compared to untreated *CLNI^{R151X}* sheep (**Figure 6B**). This correlated with our gross anatomical and imaging observations (**Figure 5**).

DISCUSSION

Devising an effective treatment strategy for CLN1 disease is a particularly difficult challenge. In addition to its early onset and rapid progression, this disorder affects widespread and anatomically distant regions of the CNS, all of which need treatment. CLN1 disease is theoretically amenable to gene therapy via CNS delivery of the *CLN1* gene via or by delivery of recombinant PPT1 enzyme via ERT to the CNS (3, 7). Although gene therapy for CLN1 disease has shown promise in preclinical studies, its effects are relatively localized and has been less effective than for CLN2 disease (23). At present, there remain limitations for the immediate clinical translation of gene therapy including transduction efficiency, immune response to viral vectors and appropriate routes of administration to maximise biodistribution (29-31), and work is ongoing to overcome these obstacles. We therefore reasoned that ERT, with its potential to treat the PPT1-deficient CNS, could represent a means to rapid and potentially more effective translation, despite potential challenges such as the need for repeated enzyme delivery, the attendant risk of port-associated infections, and potential immune responses to the exogenous protein (3, 32, 33). Our data show that repeated dosing of rhPPT1 can serve as an effective enzyme replacement strategy for CLN1 disease, with demonstrable efficacy across both small and large animal models of this fatal disorder.

Having prepared rhPPT1 with favorable uptake properties, the key to the success of our ERT strategy for CLN1 disease was devising how to deliver this enzyme. This needs to be in sufficient amounts to improve disease outcomes in both the brain and spinal cord (15, 23). Such enzyme administration to the CSF could plausibly be achieved by either intracerebroventricular or intrathecal delivery. We reasoned that dosing rhPPT1 intrathecally would be suited to treat the significant spinal pathology that occurs in *Cln1*^{-/-} mice (15, 16,

23). While intracerebroventricular infusions would treat affected brain regions, they potentially may not effectively reach the spinal cord, although our data suggest that ICV delivery does in fact reach the lumbar spinal cord of sheep relatively quickly (Supplementary Figure S6B). Nevertheless, based on our previous gene therapy study in mice (23), we opted to test the potential of either route of administration we compared intracerebroventricular and intrathecal rhPPT1 delivery in mice, in addition to a combined administration via both routes. Our data show that regardless of the route of delivery, repeated administration of rhPPT1 to the cerebrospinal fluid is well tolerated in *Cln1^{-/-}* mice. However, compared to intracerebroventricular delivery, there was less overall therapeutic benefit upon the brain after intrathecal rhPPT1 delivery. Splitting the same total dose of rhPPT1 across both delivery routes was also less effective against all outcome measures, suggesting that a certain threshold of rhPPT1 activity must be reached for ERT to be effective. Taken together, our *Cln1^{-/-}* mouse data reveal that intracerebroventricular administration alone provides sufficient rhPPT1 biodistribution to reach both the brain and spinal cord. This is consistent with the greater efficacy of intracerebroventricular rhPPT1 infusions in *Cln1^{-/-}* mice upon both motor performance and pathological outcome measures.

Although mouse models provide a valuable testing ground for preclinical strategies, many promising approaches fail to be translated into successful clinical treatments. This is not surprising given the considerable differences in the relative complexity and physical size of the CNS between mice and humans, in addition to considerable species differences in drug metabolism (6). Large animal models represent a crucial intermediate test system that is well suited to determine how to adapt drug delivery and dosing to successfully treat a larger and more complex CNS. This approach was successful in the preclinical testing of intracerebroventricular enzyme replacement therapy for the late-infantile form of neuronal

ceroid lipofuscinosis, CLN2 disease (22, 34, 35). This led to the first FDA-approved disease-limiting therapy for any neuronopathic lysosomal storage disorder (6). Such preclinical studies in either dogs or sheep have mostly relied upon naturally occurring mutants. However, the advent of modern gene editing methods such as CRISPR/Cas9 allowed us to generate a *CLNI^{R151X}* sheep model with a common human disease-causing mutation (20). This model was specifically created for the purpose of testing how to scale up preclinical strategies that show efficacy in *Cln1^{-/-}* mice for human translation. This sheep model also allowed us to test outcome measures that might feasibly be used in a subsequent human clinical trial. We are still developing suitable neurological outcome assessment measurements for use in *CLNI^{R151X}* sheep (20), including maze testing of cognitive function and other neurological tests similar to those performed in naturally occurring NCL sheep models (36, 37). However, our data revealed that quantitative MRI can detect treatment effects in sheep using a widely available human clinical MRI system with a standard clinical sequence and a widely used and validated human post-processing approach. This is encouraging for the subsequent use of such an imaging methodology in children with CLN1 disease (38).

The demonstrable efficacy of rhPPT1 across both mouse and sheep models of CLN1 disease indicates the value of such a cross-species approach for developing a successful treatment strategy. While this study is focused on a single rare disorder, this approach has broader applicability for developing therapies for a range of similar conditions. Enzyme replacement therapy with rhPPT1 successfully attenuates disease progression in *Cln1^{-/-}* mice and *CLNI^{R151X}* sheep. As early diagnosis of CLN1 disease becomes more feasible, having an effective means to intervene therapeutically would completely alter clinical practice. In order to achieve complete “normalization” of disease, achieving a sustained and higher concentration of PPT1 in the central nervous system may be required. Increasing the

frequency of enzyme infusions or administering a higher dose of enzyme are strategies that can achieve this, at least acutely, in *Cln1*^{-/-} mice (Supplementary Figure S1C) and it will be important to test this in chronic treatment studies. Alternatively, the cellular uptake of PPT1 could be further improved by engineering a highly phosphorylated version, as has been shown *in vitro* for other lysosomal enzymes (39). It is also possible that initiating treatment earlier, using recombinant sheep PPT1 or using an alternate cell line to produce enzyme may further improve efficacy in *CLN1*^{R151X} sheep. In addition, it will also be important to treat other affected organs such as the eye and other sites outside the CNS, which are unlikely to be treated effectively by intracerebroventricular rhPPT1 delivery.

Overall, we have shown that repeated dosing of ERT in CLN1 disease can be a viable therapeutic strategy, and that the cross-species pipeline with defined outcome measures will facilitate dosing and biodistribution studies, representing a significant step forward towards a clinical therapy as there is currently no FDA-approved treatment for this fatal disease.

MATERIALS AND METHODS

Study Design

The goal of this study was to test the efficacy of repeated delivery of 20 µg of rhPPT1 enzyme to the CNS of PPT1-deficient mice (*Cln1*^{-/-}) and sheep (*CLN1*^{R151X}). First, *Cln1*^{-/-} mice were given monthly infusions of rhPPT1 enzyme starting at postnatal day 1 (P1) via intracerebroventricular (ICV), Intrathecal (IT) or combined ICV+IT (split dose) routes for 6 months, with appropriate controls – vehicle treated *Cln1*^{-/-} mice and naïve wild-type mice. ICV infusions from P30 were via a chronic cannula placed in the left ventricle. Mice were assessed at monthly intervals for changes in motor performance using semi-automated gait

analysis and rotarod paradigms. At 6 months (disease end-stage), mice were sacrificed and collected tissue analyzed for enzymatic activity and neuropathology. All analyses were performed blind to genotype and treatment. Having established the most effective route of rhPPT1 administration in mice, *CLNI^{R151X}* sheep starting at 6 months of age were given monthly infusions of rhPPT1 or vehicle for 7 months via a surgically implanted ICV cannula. At 13 months, sheep were sacrificed, underwent MRI within 1 hour of sacrifice and tissue subsequently collected for biochemical and histopathological analysis. An acute dose response study was also performed in 2 month old *Cln1^{-/-}* mice to determine whether delivering a higher, 40 µg, dose of rhPPT1 would further increase CNS levels of PPT1 activity above those seen with a 20 µg dose.

Animals

Congenic *Cln1^{-/-}* and wild-type (WT) mice were previously engineered at the University of Texas Southwestern Medical Center, Dallas, TX (19), and were maintained on a C57Bl/6J background. *CLNI^{R151X}* sheep were previously engineered at the Roslin Institute, University of Edinburgh, Easter Bush, Scotland, UK (20), and were now generated by breeding heterozygous sheep. Homozygous *CLNI^{R151X}* sheep were confirmed by appropriate genotyping (20). See Supplementary methods for further details.

rhPPT1 Enzyme formulation and administration

The rhPPT1 used in this study is identical to that previously produced and purified using Chinese Hamster Ovary (CHO) cells as described (17), and characterized by Western blotting. Purified PPT1 was tested by CIMPR binding assay for affinity to the immobilized cation independent mannose-6-phosphate receptor (CI-MPR) and the half-maximal binding

(Kd) was determined as described (17). Glycopeptide composition (glycosylation and phosphorylation) was determined by liquid chromatography high resolution mass spectrometry (LC-UV-HRMS), as described (17). All mice, regardless of route of administration (ICV, IT, ICV+IT) received the same total dose of enzyme – 5 µl of rhPPT1 at 4 mg/ml, as monthly infusions for 6 months. 6-month-old *CLNI^{R151X}* sheep received 1 ml of the same 4 mg/ml rhPPT1 preparation, infused at a rate of 0.6 ml/hour. These infusions were given monthly starting at 6 months and ending at 13 months of age. See Supplementary methods for further details.

Murine behavioral analysis

Rotarod testing using stationary (60 sec) and constant speed (2.5 rpm) paradigms (23), and gait analysis using the *CatWalk XT* system (Noldus Information Technology) was performed as previously described (15) using n=10 mice per group at monthly intervals beginning at 1 month until 6 months. All behavioral tests were performed after appropriate habituation and training. See Supplementary methods for further details.

Ovine MRI analysis

Sheep were imaged within 1 hour of being sacrificed. Structural sequences included 3D T1-, T2-weighted and FLAIR (Fluid-attenuated inversion recovery) imaging with whole brain coverage. Apparent diffusion coefficients were calculated using RESOLVE (readout segmentation of long variable echo-trains) to minimize echoplanar distortions. The extracted brains were classified using the ANTs (advanced normalisation tools) for 3 tissue classes (cerebrospinal fluid (CSF), grey matter (GM), and white matter (WM)). Extracted brains were then co-registered to the INRA (Institut national de la recherche agronomique) brain

only template (28). Total brain volume was calculated from a combination of the GM and WM tissue class probability maps. All metrics were adjusted for total intracranial volume (GM+WM+CSF), total brain volume (GM+WM), and total grey matter volume. We have previously described that areas of cortical grey matter undergo differential degrees of atrophy in homozygous *CLNI^{R151X}* sheep (20) and therefore regional GM volumes were normalized to total grey matter volume to assess for relative preservation of cortical regions. See Supplementary methods for further details.

Tissue Collection and histopathological analysis

Mouse brain and spinal cord tissue were collected for biochemical and histological processing as previously described (23). Sheep tissues were collected for biochemical analyses and histological processing as previously described (20). Mouse brains and spinal cords were stained for cresyl fast violet as well as immunostained for glial markers and storage material as previously described (15). Sheep brain sections were stained using a free-floating immunofluorescence protocol for astrocytes (GFAP) and microglia (Iba-1) as well as to directly visualize autofluorescent storage material (AFSM). See Supplementary methods for further details. Cresyl fast violet stained tissue was analyzed for cortical thickness and neuron counts as before (14, 15) and immunostained tissue (and tissue for AFSM) were analyzed using thresholding image analysis as before (15). See Supplementary methods for further details.

Analysis of enzyme activity

Mouse and sheep tissue were homogenized and analyzed for PPT1 activity using the 4-MU-palmitate fluorometric assay and normalized to total protein. Secondary elevations of another

lysosomal enzyme, β -glucuronidase, were determined using the 4-MU- β -D-glucuronide fluorometric assay and normalized to total protein as previously described (23, 40).

Statistical Analysis

All measurements for histological processing were performed blind to genotype. All statistical analyses were performed using *GraphPad Prism* (GraphPad Software, San Diego, California USA). Gait and rotarod data were analyzed using a two-way ANOVA with a post-hoc Bonferroni correction and all biochemical and histological analysis were analyzed using a one-way ANOVA with a post-hoc Bonferroni correction. In all instances a p-value of ≤ 0.05 was considered significant. In all figures p values are indicated as follows - * $p \leq 0.05$, ** ≤ 0.01 , *** ≤ 0.001 and **** ≤ 0.0001 .

Study Approval

All procedures were performed in accordance with NIH guidelines under a protocol approved by the Institutional Animal Care and Use Committee (IACUC) at Washington University School of Medicine (protocols 2018-0215 and 21-0292). Sheep studies were reviewed and approved by the Animal Welfare and Ethical Review Board (AWERB) at the Roslin Institute and conducted under the authority of the UK Home Office (equivalent of IACUC). Work detailed here was carried out under license number PEF7C7DB6A.

Author contributions:

Study design: JDC, TMW, SE, MSS, HRN

Enzyme preparation: YL, SLH

Enzyme Western Blotting: ACP, SE

Biochemical characterization of Enzyme: NS

Mouse studies in vivo, behavior, biochemistry and histology: HRN, SHW, EMM, KT, SQL, RH, JT

Sheep Studies in vivo and biochemistry: SLE, GT, FM, PMB, MG, SG, PT, RG, EC JN, CP, SG, SGL, BAW, MSS

Sheep histology: HRN, SHW, KT

Funding acquisition: JDC, SE, ACP, TMW, MSS

Project administration: JDC, SE, TMW, MSS

Supervision: JDC, MSS, PID, TMW, SE

Writing – original draft: HRN, JDC, SE, ACP

Writing – review & editing: TMW, MSS, PID, SE, with input from all authors

HRN and SLE are co-first authors. Order of authorship assigned based on overall contribution and writing up of manuscript.

Acknowledgments:

The authors would like to thank Adrian Ritchie for his help with the *CLNI^{R151X}* sheep experiments; Jessie Feng, and Suresh Venkateswaran for assistance with the biochemical characterization of rhPPT1 at Amicus Therapeutics, Inc; Dr. Nathan Nicely and Dr. John Forsberg (UNC) for assistance with the rhPPT1 western blot; Dr. Marco Sardiello, Dr. David Holtzman, Dr. Marion Bonneau and Dr. Alison Barnwell for their insights and useful comments on the manuscript. For the purpose of open access, the author has applied a CC BY public copyright license to any Author Accepted Manuscript version arising from this submission

Funding:

NINDS National Institutes of Health grants R43 NS107079 (SE, JDC),
R43NS107079-01S1 (SE, ACP) and 3R43NS107079-01S2 (SE)

NINDS National Institutes of Health grants R56 NS117635 and R01 NS124655 (JDC,
TMW, MSS)

NINDS National Institutes of Health grant R01 NS100779 (MSS)

Hailey's Heroes project grant (JDC, TMW, MSS)

Biotechnology and Biological Sciences Research Council (BBSRC) BB/J004316/1
and BB/P013732/1 ISP support to The Roslin Institute (TMW, SLE)

The RS Macdonald Charitable Trust (TMW)

Institutional Support from the Department of Pediatrics, Washington University in St
Louis, School of Medicine (JDC)

McDonnell International Scholars Academy award (KT)

Conflict of interest statement:

JDC has received research support from BioMarin Pharmaceutical Inc., Abeona Therapeutics Inc., Regenxbio Inc., Neurogene and Alnylam and is a consultant for JCR Pharmaceuticals. PID receives research support from Alnylam, Genzyme, and M6P Therapeutics and is a consultant for Mandos. NS was a paid employee of Amicus Therapeutics, Inc at the time of the study; SE is the owner and ACP is an employee of Collaborations Pharmaceuticals, Inc. which also owns the FDA orphan and rare disease designations for rhPPT1. SLH was a consultant to Collaborations Pharmaceuticals, Inc. The other authors declare no competing interests.

Data and materials availability: All data are available in the main text or the supplementary materials.

References

1. Uzor NE, McCullough LD, and Tsvetkov AS. Peroxisomal Dysfunction in Neurological Diseases and Brain Aging. *Front Cell Neurosci.* 2020;14:44.
2. Wang Y, Xu E, Musich PR, and Lin F. Mitochondrial dysfunction in neurodegenerative diseases and the potential countermeasure. *CNS Neurosci Ther.* 2019;25(7):816-24.
3. Puhl AC, and Ekins S. Advancing the Research and Development of Enzyme Replacement Therapies for Lysosomal Storage Diseases. *GEN Biotechnology.* 2022;1(2):156-62.
4. Sands MS, and Davidson BL. Gene therapy for lysosomal storage diseases. *Molecular Therapy.* 2006;13(5):839-49.
5. Okuyama T, Eto Y, Sakai N, Nakamura K, Yamamoto T, Yamaoka M, et al. A Phase 2/3 Trial of Pabinafusp Alfa, IDS Fused with Anti-Human Transferrin Receptor Antibody, Targeting Neurodegeneration in MPS-II. *Mol Ther.* 2021;29(2):671-9.
6. Schulz A, Ajayi T, Specchio N, de Los Reyes E, Gissen P, Ballon D, et al. Study of Intraventricular Cerliponase Alfa for CLN2 Disease. *New England Journal of Medicine.* 2018;378(20):1898-907.
7. Mole SE, Anderson G, Band HA, Berkovic SF, Cooper JD, Kleine Holthaus S-M, et al. Clinical challenges and future therapeutic approaches for neuronal ceroid lipofuscinosis. *The Lancet Neurology.* 2019;18(1):107-16.
8. Warriar V, Vieira M, and Mole SE. Genetic basis and phenotypic correlations of the neuronal ceroid lipofuscinoses. *Biochimica et Biophysica Acta (BBA) - Molecular Basis of Disease.* 2013;1832(11):1827-30.
9. Gardner E, and Mole SE. The Genetic Basis of Phenotypic Heterogeneity in the Neuronal Ceroid Lipofuscinoses. *Front Neurol.* 2021;12:754045.

10. Augustine EF, Adams HR, de Los Reyes E, Drago K, Frazier M, Guelbert N, et al. Management of CLN1 Disease: International Clinical Consensus. *Pediatr Neurol.* 2021;120:38-51.
11. Kohlschütter A, Schulz A, Bartsch U, and Storch S. Current and Emerging Treatment Strategies for Neuronal Ceroid Lipofuscinoses. *CNS Drugs.* 2019;33(4):315-25.
12. Johnson TB, Cain JT, White KA, Ramirez-Montealegre D, Pearce DA, and Weimer JM. Therapeutic landscape for Batten disease: current treatments and future prospects. *Nature Reviews Neurology.* 2019;15(3):161-78.
13. Vesa J, Hellsten E, Verkruyse LA, Camp LA, Rapola J, Santavuori P, et al. Mutations in the palmitoyl protein thioesterase gene causing infantile neuronal ceroid lipofuscinosis. *Nature.* 1995;376(6541):584-7.
14. Kielar C, Maddox L, Bible E, Pontikis CC, Macauley SL, Griffey MA, et al. Successive neuron loss in the thalamus and cortex in a mouse model of infantile neuronal ceroid lipofuscinosis. *Neurobiology of Disease.* 2007;25(1):150-62.
15. Nelvagal HR, Dearborn JT, Ostergaard JR, Sands MS, and Cooper JD. Spinal manifestations of CLN1 disease start during the early postnatal period. *Neuropathol Appl Neurobiol.* 2021;47(2):251-67.
16. Lu J-Y, Nelvagal HR, Wang L, Birnbaum SG, Cooper JD, and Hofmann SL. Intrathecal enzyme replacement therapy improves motor function and survival in a preclinical mouse model of infantile neuronal ceroid lipofuscinosis. *Molecular Genetics and Metabolism.* 2015;116(1-2):98-105.
17. Lu J-Y, Hu J, and Hofmann SL. Human recombinant palmitoyl-protein thioesterase-1 (PPT1) for preclinical evaluation of enzyme replacement therapy for infantile neuronal ceroid lipofuscinosis. *Molecular Genetics and Metabolism.* 2010;99(4):374-8.

18. Hu J, Lu J-Y, Wong AMS, Hynan LS, Birnbaum SG, Yilmaz DS, et al. Intravenous high-dose enzyme replacement therapy with recombinant palmitoyl-protein thioesterase reduces visceral lysosomal storage and modestly prolongs survival in a preclinical mouse model of infantile neuronal ceroid lipofuscinosis. *Molecular Genetics and Metabolism*. 2012;107(1-2):213-21.
19. Gupta P, Soyombo AA, Atashband A, Wisniewski KE, Shelton JM, Richardson JA, et al. Disruption of PPT1 or PPT2 causes neuronal ceroid lipofuscinosis in knockout mice. *Proceedings of the National Academy of Sciences of the United States of America*. 2001;98(24):13566-71.
20. Eaton SL, Proudfoot C, Lilloco SG, Skehel P, Kline RA, Hamer K, et al. CRISPR/Cas9 mediated generation of an ovine model for infantile neuronal ceroid lipofuscinosis (CLN1 disease). *Scientific Reports*. 2019;9(1):9891-.
21. Vuillemenot BR, Katz ML, Coates JR, Kennedy D, Tiger P, Kanazono S, et al. Intrathecal tripeptidyl-peptidase 1 reduces lysosomal storage in a canine model of late infantile neuronal ceroid lipofuscinosis. *Molecular Genetics and Metabolism*. 2011;104(3):325-37.
22. Vuillemenot BR, Kennedy D, Cooper JD, Wong AMS, Sri S, Doeleman T, et al. Nonclinical evaluation of CNS-administered TPP1 enzyme replacement in canine CLN2 neuronal ceroid lipofuscinosis. *Molecular Genetics and Metabolism*. 2015;114(2):281-93.
23. Shyng C, Nelvagal HR, Dearborn JT, Tyynela J, Schmidt RE, Sands MS, et al. Synergistic effects of treating the spinal cord and brain in CLN1 disease. *Proc Natl Acad Sci U S A*. 2017;114(29):E5920-E9.
24. Griffey M, Bible E, Vogler C, Levy B, Gupta P, Cooper J, et al. Adeno-associated virus 2-mediated gene therapy decreases autofluorescent storage material and

- increases brain mass in a murine model of infantile neuronal ceroid lipofuscinosis. *Neurobiology of Disease*. 2004;16(2):360-9.
25. Griffey M, Macauley SL, Ogilvie JM, and Sands MS. AAV2-mediated ocular gene therapy for infantile neuronal ceroid lipofuscinosis. *Molecular Therapy*. 2005;12(3):413-21.
 26. Macauley SL, Wozniak DF, Kielar C, Tan Y, Cooper JD, and Sands MS. Cerebellar pathology and motor deficits in the palmitoyl protein thioesterase 1-deficient mouse. *Experimental Neurology*. 2009;217(1):124-35.
 27. Kühl TG, Dihanich S, Wong AMS, and Cooper JD. Regional Brain Atrophy in Mouse Models of Neuronal Ceroid Lipofuscinosis. *Journal of Child Neurology*. 2013;28(9):1117-22.
 28. Ella A, Delgadillo JA, Chemineau P, and Keller M. Computation of a high-resolution MRI 3D stereotaxic atlas of the sheep brain. *J Comp Neurol*. 2017;525(3):676-92.
 29. Maguire CA, Ramirez SH, Merkel SF, Sena-Esteves M, and Breakefield XO. Gene therapy for the nervous system: challenges and new strategies. *Neurotherapeutics*. 2014;11(4):817-39.
 30. Pena SA, Iyengar R, Eshraghi RS, Bencie N, Mittal J, Aljohani A, et al. Gene therapy for neurological disorders: challenges and recent advancements. *J Drug Target*. 2020;28(2):111-28.
 31. Mendell JR, Al-Zaidy SA, Rodino-Klapac LR, Goodspeed K, Gray SJ, Kay CN, et al. Current Clinical Applications of In Vivo Gene Therapy with AAVs. *Mol Ther*. 2021;29(2):464-88.
 32. Edelmann MJ, and Maegawa GHB. CNS-Targeting Therapies for Lysosomal Storage Diseases: Current Advances and Challenges. *Front Mol Biosci*. 2020;7:559804.

33. Concolino D, Deodato F, and Parini R. Enzyme replacement therapy: efficacy and limitations. *Ital J Pediatr.* 2018;44(Suppl 2):120.
34. Katz ML, Coates JR, Sibigtroth CM, Taylor JD, Carpentier M, Young WM, et al. Enzyme replacement therapy attenuates disease progression in a canine model of late-infantile neuronal ceroid lipofuscinosis (CLN2 disease). *Journal of Neuroscience Research.* 2014;92(11):1591-8.
35. Chang M, Cooper JD, Sleat DE, Cheng SH, Dodge JC, Passini MA, et al. Intraventricular Enzyme Replacement Improves Disease Phenotypes in a Mouse Model of Late Infantile Neuronal Ceroid Lipofuscinosis. *Molecular Therapy.* 2008;16(4):649-56.
36. Cronin GM, Beganovic DF, Sutton AL, Palmer D, Thomson PC, and Tammen I. Manifestation of neuronal ceroid lipofuscinosis in Australian Merino sheep: observations on altered behaviour and growth. *Appl Anim Behav Sci.* 2016;175:32-40.
37. Mitchell NL, Russell KN, Wellby MP, Wicky HE, Schoderboeck L, Barrell GK, et al. Longitudinal In Vivo Monitoring of the CNS Demonstrates the Efficacy of Gene Therapy in a Sheep Model of CLN5 Batten Disease. *Mol Ther.* 2018;26(10):2366-78.
38. Vanhanen SL, Puranen J, Autti T, Raininko R, Liewendahl K, Nikkinen P, et al. Neuroradiological Findings (MRS, MRI, SPECT) in Infantile Neuronal Ceroid-Lipofuscinosis (Infantile CLN1) at Different Stages of the Disease. *Neuropediatrics.* 2004;35(01):27-35.
39. Liu L, Lee WS, Doray B, and Kornfeld S. Engineering of GlcNAc-1-Phosphotransferase for Production of Highly Phosphorylated Lysosomal Enzymes for Enzyme Replacement Therapy. *Mol Ther Methods Clin Dev.* 2017;5:59-65.

40. Sands MS, Vogler C, Kyle JW, Grubb JH, Levy B, Galvin N, et al. Enzyme replacement therapy for murine mucopolysaccharidosis type VII. *J Clin Invest.* 1994;93(6):2324-31.

Figures

hPPT1 enzyme characterization

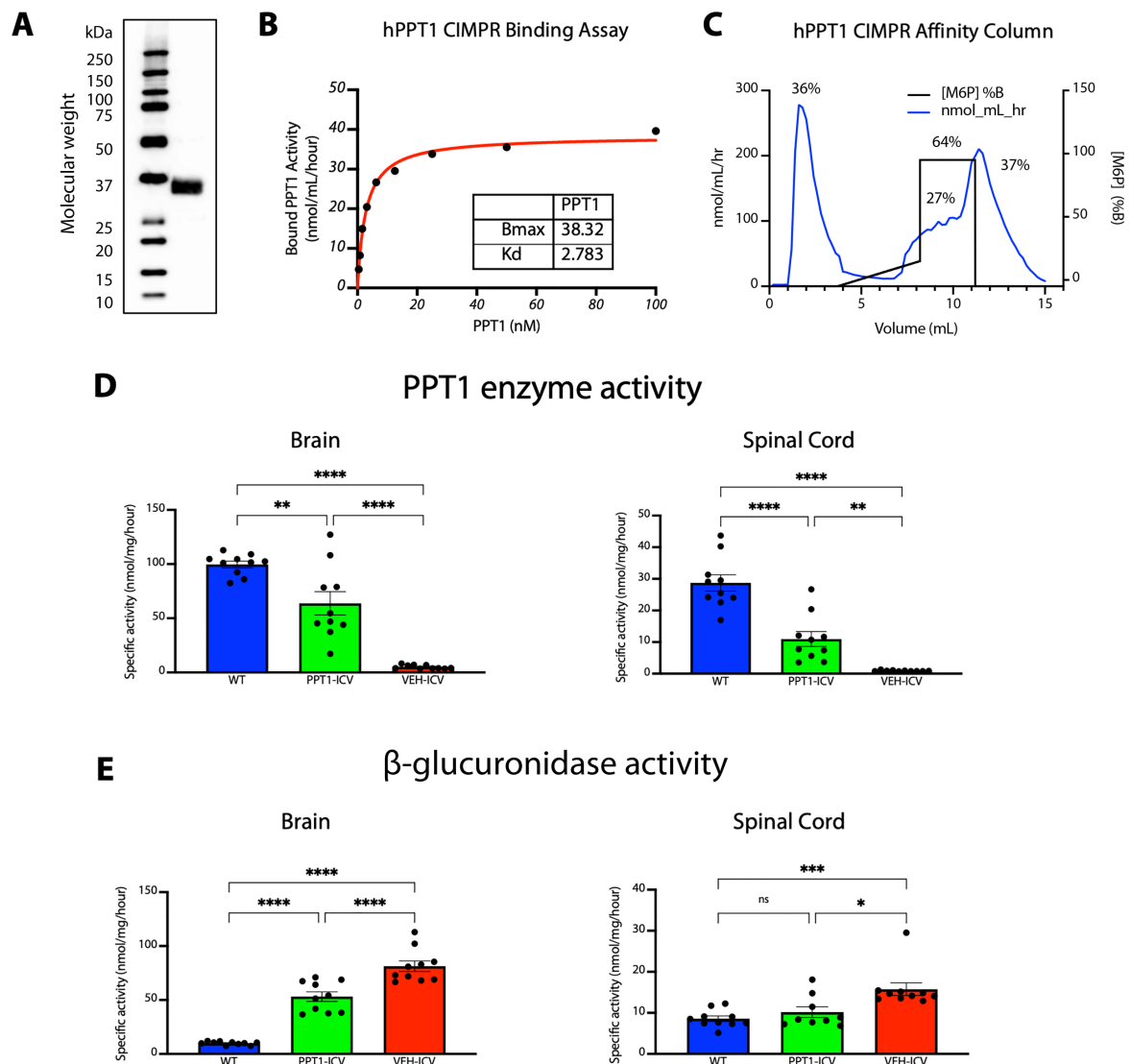


Figure 1. rhPPT1 enzyme characterization and *in vivo* efficacy in *Cln1*^{-/-} mice.

(A) Representative western blot image of staining for PPT1 protein (~37kDa) from CHO cell lysates (Full gel in Figure S7). rhPPT1 binding assay to immobilized cation independent mannose-6-phosphate receptor (CI-MPR), showing the half-maximal binding (K_d) of rhPPT1 at 2.78 nM and maximum binding (B_{max}) at 38.32 nM (B) and that 64% of loaded rhPPT1 remain bound to affinity column (C). Specific activity in nmol/mg/h of PPT1 (D) and β -glucuronidase (E) enzymes from homogenates collected from mice 24 hours after their last

intracerebroventricular (ICV) infusion showing statistically significantly increased PPT1 activity and reduced β -glucuronidase activity in both the brain and spinal cord of treated mice (PPT1-ICV) as compared to vehicle treated controls (VEH-ICV). However, these enzyme values were not normalized to levels in wild-type (WT) control mice. Data represent mean \pm SEM. One-Way ANOVA with *post-hoc* Bonferroni correction. n=10; *p<0.05, **p<0.01, ***p<0.001, ****p<0.0001 (See Data File S2 for full p values).

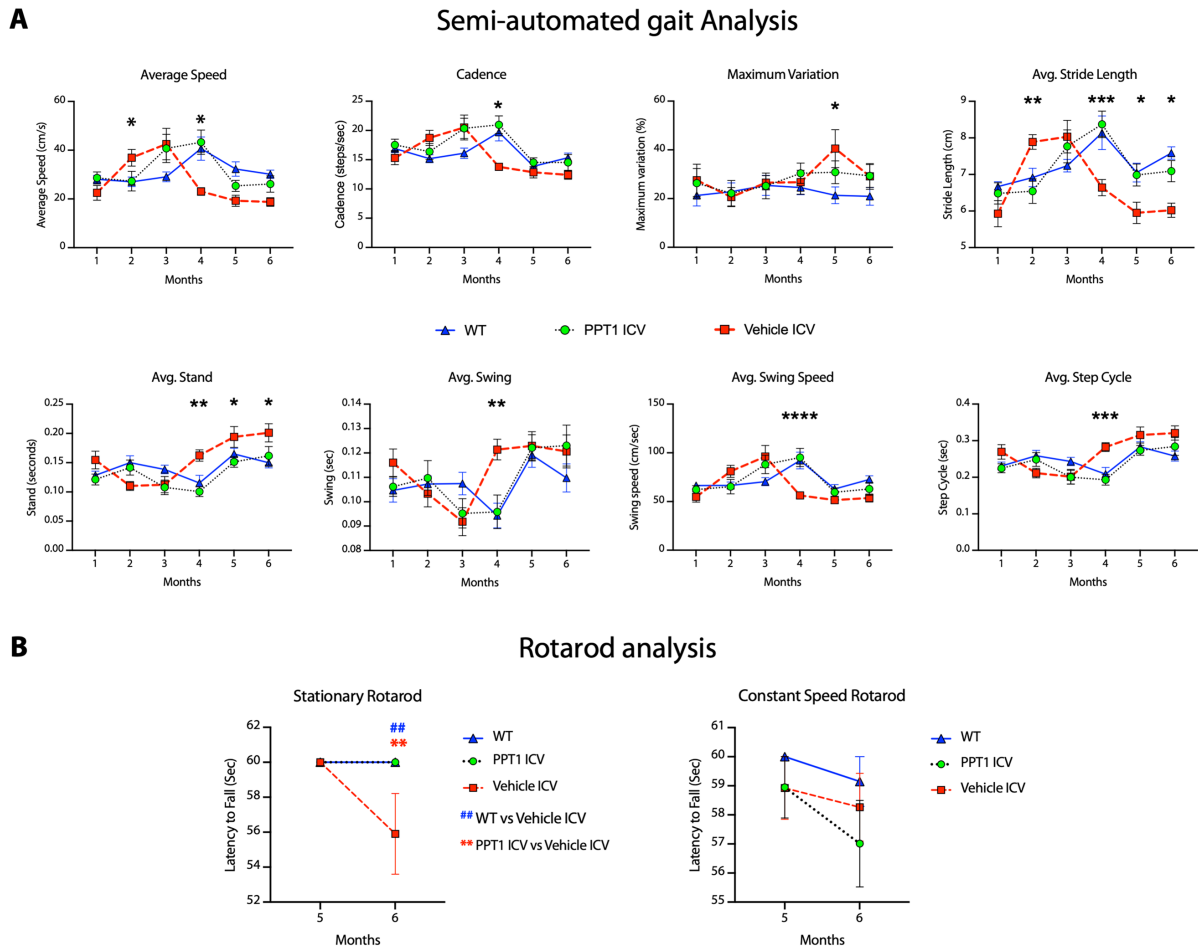


Figure 2. Improved motor performance in ICV treated *Cln1*^{-/-} mice.

(A) Semi-automated gait analysis measures of average speed (cm/s), cadence (steps/second), maximum variation of speed (%), Stride length (cm), Stand (s), Swing (s), Swing speed (cm/s) and step cycle (s) from 1-6 months showing overall improved performance of intracerebroventricular treated (PPT1-ICV) mice compared to vehicle treated (Vehicle ICV), and similar to wild-type (WT) values. (B) Stationary and constant-speed rotarod tests in 5- and 6- month old mice. PPT1-ICV mice showed similar performance to WT while Vehicle ICV mice showed a statistically significant reduction in latency to fall (s) in the stationary rotarod test at 6 months. Both PPT1-ICV and Vehicle ICV mice showed a reduced latency to fall at 6 months in constant speed rotarod test, but this did not reach statistical significance. Data represent mean \pm SEM. Two-way ANOVA (mixed-effects) with *post-hoc* Bonferroni

correction. $n=10$; * $p<0.05$, ** $p<0.01$, *** $p<0.001$, **** $p<0.0001$ (See Data File S2 for full p values).

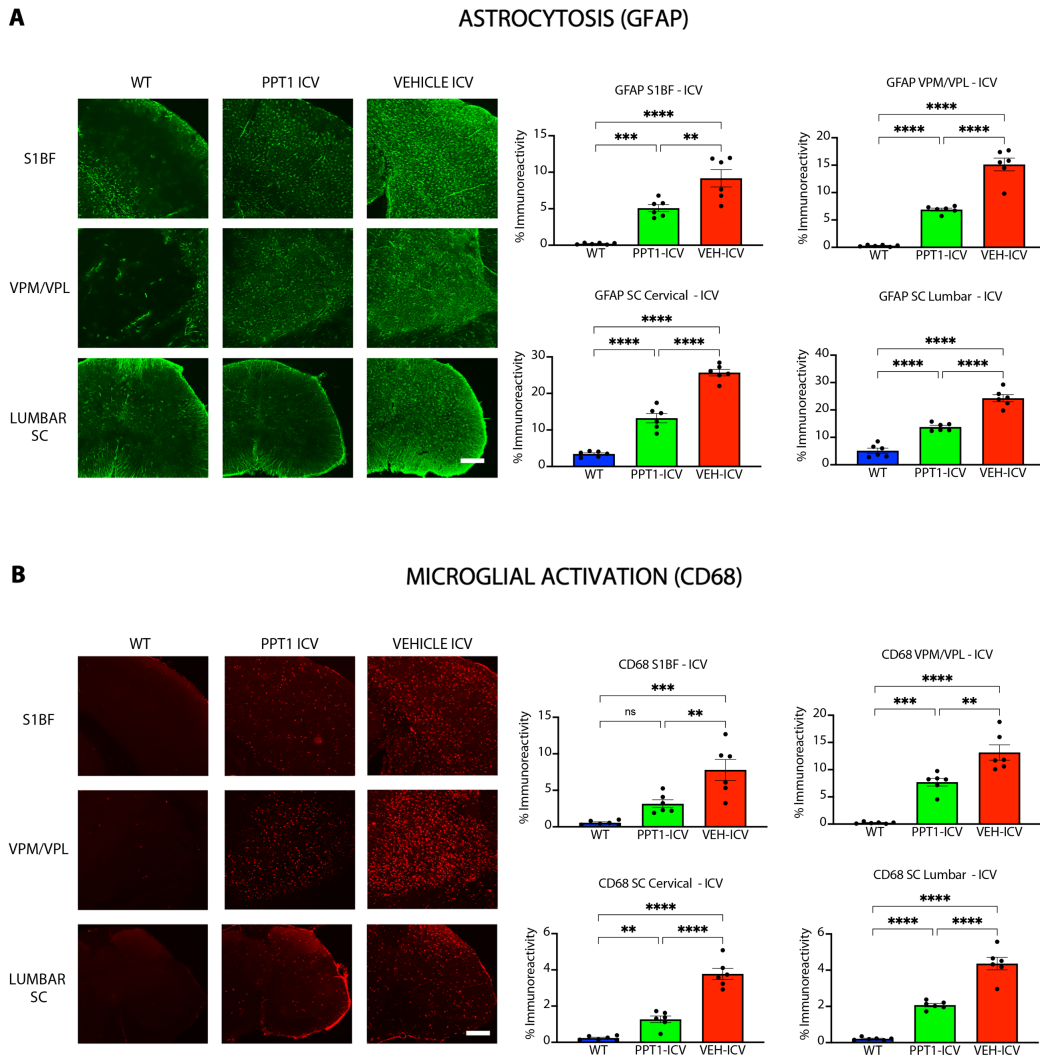


Figure 3 Decreased astrocytosis and microglial activation in brain and spinal cord of ICV treated *Cln1*^{-/-} mice.

Representative immunofluorescence images and thresholding image analysis showing an overall statistically significant reduction in (A) astrocytosis (GFAP) and (B) microglial activation (CD68) in ICV treated (PPT1 ICV) mice compared to vehicle treated (VEH ICV) mice across the primary somatosensory cortex (S1BF), ventral-posterior thalamic nucleus (VPM/VPL) and cervical and lumbar spinal cord (SC). However, these did not reach wild-type (WT) levels across any of the regions except for CD68 in S1BF. Scale Bar = 100 μ m. Data represent mean \pm SEM. One-Way ANOVA with *post-hoc* Bonferroni correction. n=6;

ns = not significant, ** $p < 0.01$, *** $p < 0.001$, **** $p < 0.0001$ (See Data File S2 for full p values).

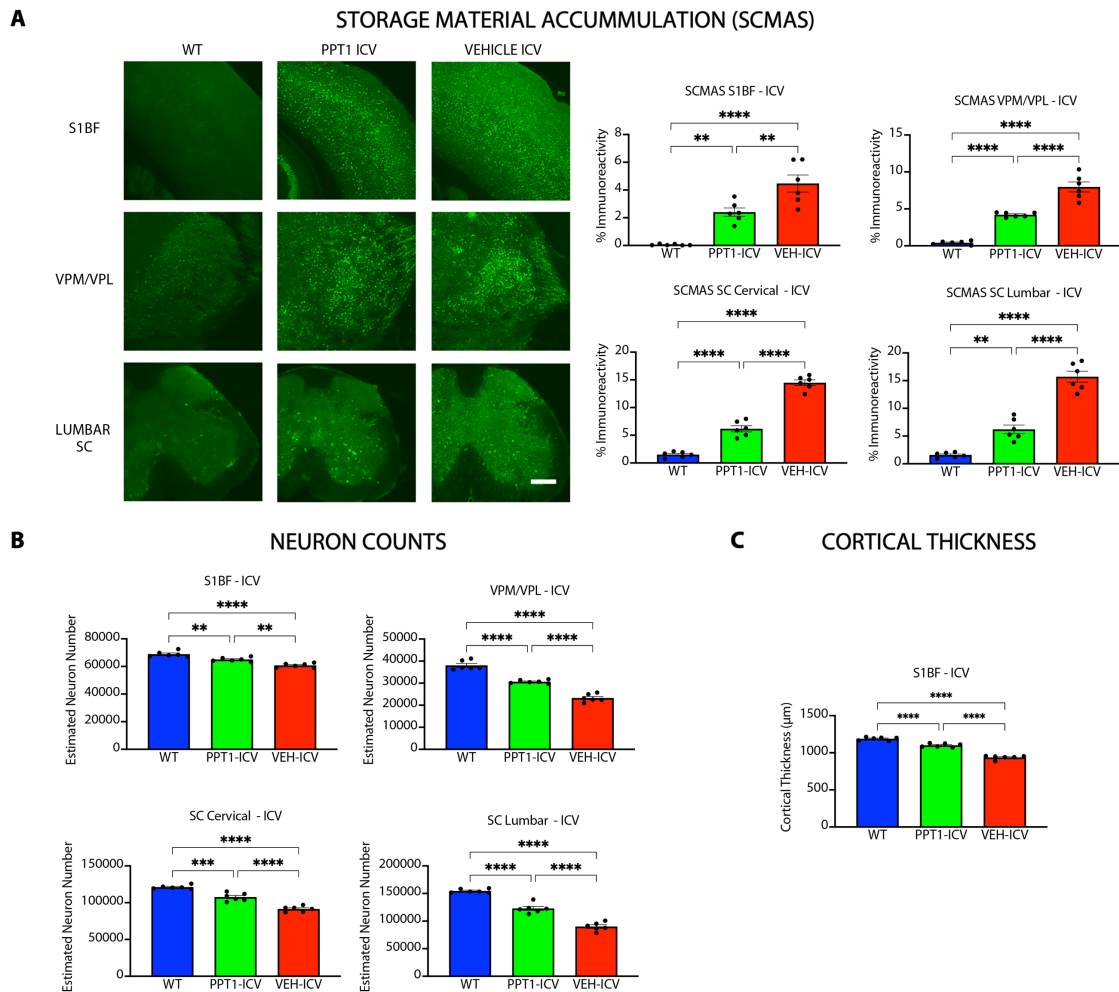


Figure 4. Decreased storage material accumulation, improved neuron survival and cortical atrophy ICV treated *Cln1*^{-/-} mice.

(A) Representative immunofluorescence images and thresholding image analysis for subunit C of mitochondrial ATPase (SCMAS) showing an overall statistically significant reduction in ICV treated (PPT1-ICV) mouse brains and cords compared to vehicle treated (VEH-ICV) mice across the primary somatosensory cortex (S1BF), ventral-posterior thalamic nucleus (VPM/VPL) and cervical and lumbar spinal cord (SC). However, these did not reach wild-type (WT) levels across any of the regions. Scale Bar = 100 μ m. Statistically significant improvements in (B) Neuron Counts across all regions and (C) Cortical atrophy (S1BF) in PPT1-ICV mice compared to VEH-ICV mice, but not completely normalized to values in

WT mice. Data represent mean \pm SEM. One-Way ANOVA with *post-hoc* Bonferroni correction. n=6; ns = not significant, **p<0.01, ***p<0.001, ****p<0.0001 (See Data File S2 for full p values).

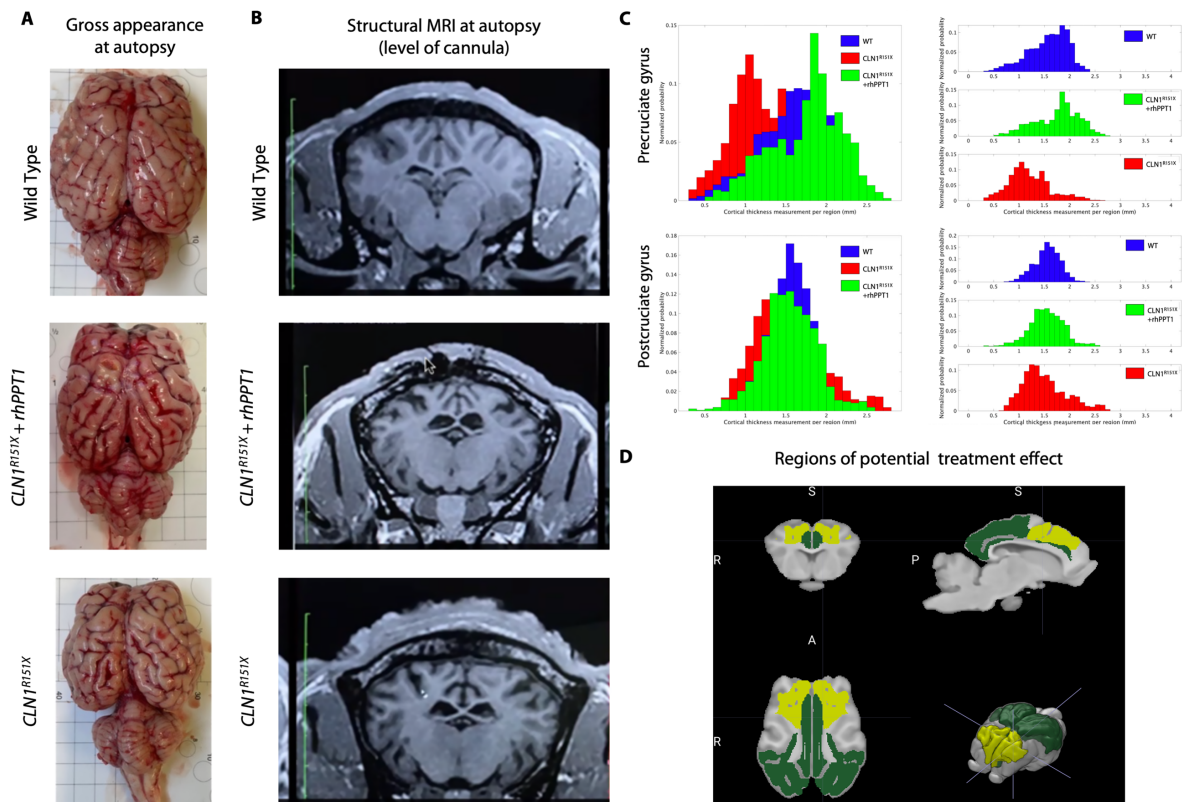


Figure 5. Therapeutic effect of ICV administration of rhPPT1 in CLN1^{R151X} sheep

(A) Gross anatomical examination and (B) structural MRI analysis showed a positive treatment effect of ICV administration of rhPPT1 (CLN1^{R151X} +rhPPT1) compared to untreated CLN1^{R151X} sheep and wild-type controls showing overall reduced cerebral and cerebellar atrophy in rhPPT1-treated CLN1^{R151X} sheep. (C) Histograms of individual measures of cortical thickness in the pre- and postcruciate gyri showing the extent of treatment effect in these regions, with the movement of values in rhPPT1-treated CLN1^{R151X} sheep (green) moving closer to values from wild-type sheep (blue), than to untreated CLN1^{R151X} controls. (See Table 1, Data File S1 for all Cortical thicknesses) (D) Solid 3D representation showing colored INRA ovine atlas (24) cortical regions in which a significant treatment effect upon individual thickness measurements was detected. ANOVA (ERT > untreated, $p < 0.0001$). Different colors indicating the magnitude of this effect, with gray regions where no significant treatment effect was detected. Yellow indicates regions where

mean cortical thickness values of rhPPT1-treated CLN1^{R151X} sheep are closer to WT values (greater treatment effect) and green those in which these values are closer to untreated CLN1^{R151X} sheep (positive treatment effect).

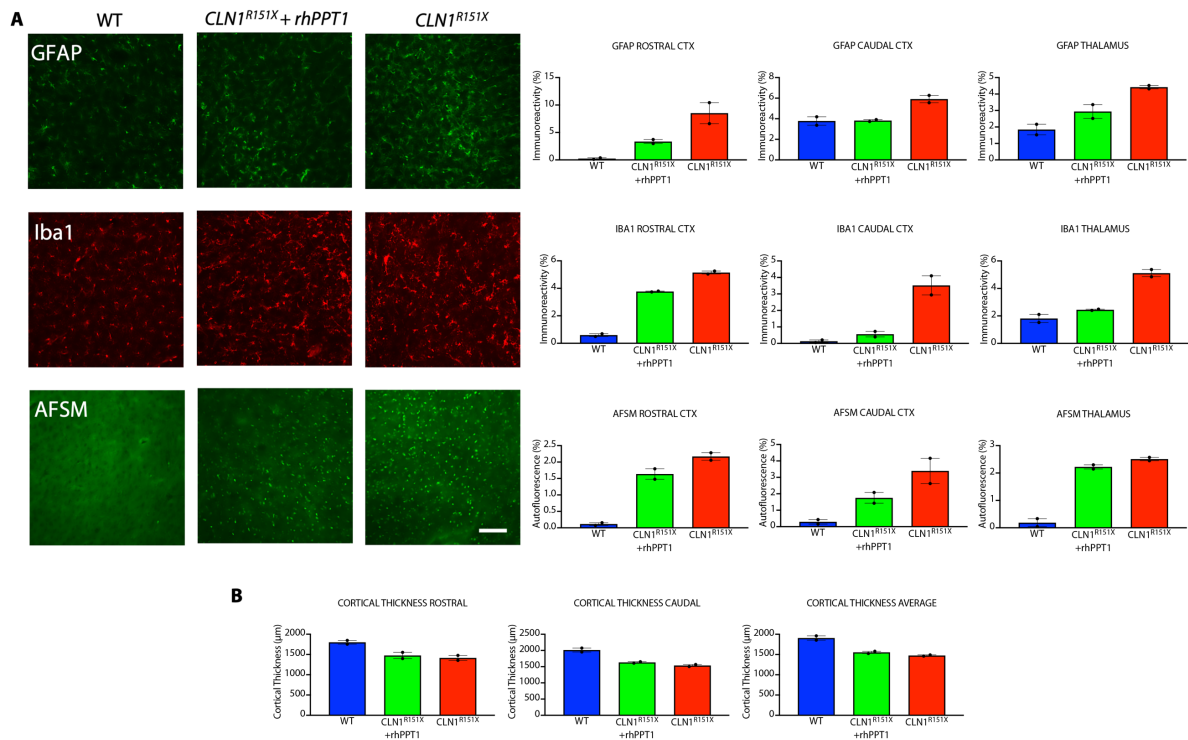


Figure 6. Therapeutic effect of ICV administration of rhPPT1 in CLN1^{R151X} sheep on neuropathology.

(A) Representative immunofluorescence images from the cortex and thresholding imaging analysis (n=2) of wild-type (WT), ICV rhPPT1 Treated (CLN1^{R151X} +rhPPT1) and untreated CLN1^{R151X} sheep showing a reduction in markers for astrocytosis (GFAP), microglial activation (CD68) and autofluorescent storage material (AFSM) accumulation across rostral and caudal regions of the somatosensory cortex as well as the thalamus. There is a reduction across all the markers in rhPPT1-treated CLN1^{R151X} sheep compared to untreated CLN1^{R151X} sheep, although these did not reach WT levels. Scale Bar=50µm. (B) Measurements of cortical thickness in rostral and caudal somatosensory cortex (and averaged values) showing slightly increased values in rhPPT1-treated CLN1^{R151X} sheep compared to untreated CLN1^{R151X}sheep. Data represent mean ± SEM .